18. Meremonte, M. *et al.* Urban seismology—Northridge after shocks recorded by multiscale arrays of portable digital seismographs. *Bull Seismol. Soc. Am.* **86,** 1350–1363 (1996).
19. Data Center of the Southern California Earthquake Center (web address: http://www.scecdc.scec.org.).

Acknowledgements. We thank several members of the Los Alamos National Laboratory (LANL) and the Southern California Earthquake Centre (SCEC) for comments and discussions. The data used in this study were collected by the SCEC, the United States Geological Survey, the California Division of Mines and Geology, the University of Southern California, the Department of Energy, and the City of Los Angeles. This work was supported by LANL Institutional Support (LDRD-IP). E.H.F. received additional support from the SCEC.

Correspondence and requests for materials should be addressed to E.H.F. (e-mail: field@usc.edu).

Absence of contour linking in peripheral vision

Robert F. Hess & Steven C. Dakin

McGill Vision Research, Department of Ophthalmology, McGill University, Montreal, Quebec, H3A 1A1 Canada

Human foveal vision is subserved initially by groups of spatial, temporal and orientational 'filters', the outputs of which are combined to define perceptual objects. Although a great deal is known about the filtering properties of individual cortical cells, relatively little is known about the nature of this 'linking' process. One recent approach[1] has shown that the process can be thought of in terms of an association field whose strength is determined conjointly by the orientation and distance of the object. Here we describe a fundamental difference in this feature-linking process in central and peripheral parts of the visual field, which provides insight into the ways that foveal and peripheral visual perception differ[2,3]. In the fovea, performance can be explained only by intercellular linking operations whereas in the periphery intracellular filtering will suffice. This difference represents a substantial economy in cortical neuronal processing of peripheral visual information and may allow a recent theory of intercellular binding to be tested[4–7].

The way that distributed neuronal activity in the cortex is combined to define perceptual objects is an important question in neurobiology[7]. In human vision, one promising method of study involves the detection of paths of spatially narrowband elements embedded in a field of similar elements with random position and orientation[1]. The elements forming the path differ from those of the background in that they conform to first-order curves (Fig. 1). Human detection performance is nearly perfect for paths with orientation differences between neighbouring elements of up to 20–30 degrees (Fig. 1a). It has been claimed[1], but never substantiated, that such performance could not be supported solely by individual cortical filters, and hence requires an integrative or linking process between cells analysing different orientations. We find that this claim is indeed correct.

We used a path-detection model operating on multiple, independent oriented filter outputs (Fig. 2 and Methods). The image is initially orientation-filtered at a scale appropriate to the elements. After thresholding, a symbolic description of the resulting orientation features is computed (a two-dimensional adaptation of the MIRAGE algorithm[8]). The path is then indicated by the longest feature present across all orientations. In the example in Fig. 2 the path angle is zero and filters aligned with the straight path correctly encode the path perceived in Fig. 2.

The solid line in Fig. 3a represents the output of our filter model, compared with the performance of human foveal vision. Model performance is much worse than that of human subjects when path angle is increased and when the paths become more curved (Fig. 3a). We could find no method of improving the performance of the model without introducing interactions between cells tuned to different orientations, providing a quantitative demonstration that filtering alone (intracellular processing), at any one of a number of orientations, is insufficient to explain human performance. A direct test of this conclusion is to use paths composed of elements whose spatial phases are alternately switched by 180°, embedded in a background of elements with spatial phase set randomly to either 0° or 180°. Such a stimulus (Fig. 1b), which cannot be detected by a simple linear filtering operation (model results are shown as a solid

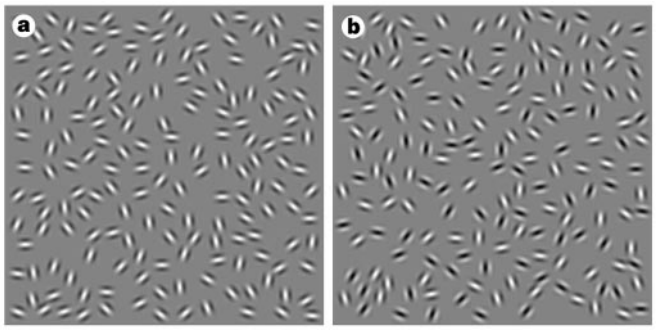

Figure 1 An example of the path stimuli used. **a**, All elements are localized in spatial frequency and are of cosine phase. The path, which is slightly curved, runs from bottom to top through the middle of the picture. **b**, A similar path, but now composed of similar elements alternating in spatial phase by 180°, curves from the bottom left to the top right, embedded in a background field of alternating-phase elements. In the fovea both types of path are easily detected, but in the periphery, the path shown in **b** is invisible.

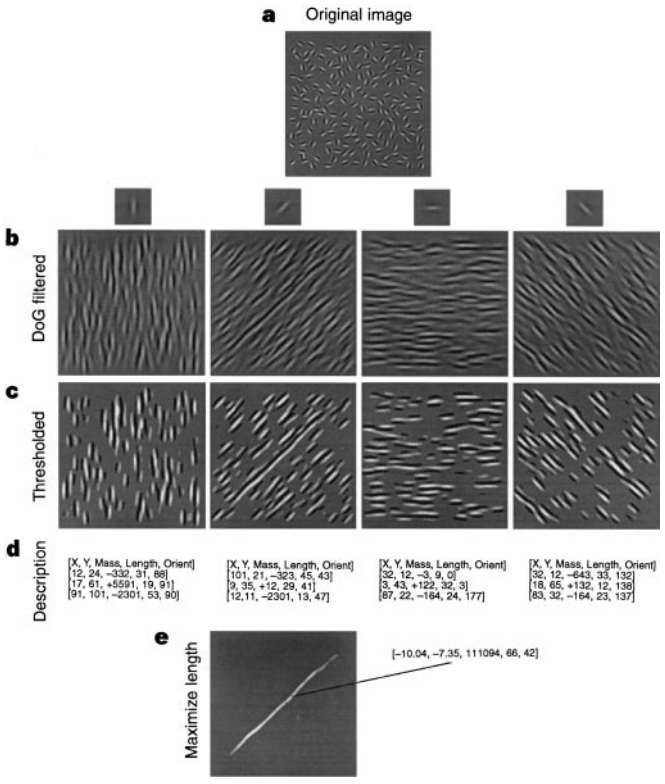

Figure 2 The simple-filter model. **a**, An example image. **b**, The operation of four filters from the full bank of 12 is shown. **c**, These filter outputs are 'thresholded' (all grey levels falling within ±1 s.d. of the mean are replaced with the mean value), producing a new image containing both positive and negative polarity 'blobs' (here blobs have been contrast-enhanced to demarcate them further). **d**, Descriptions of the 'blobs' in each of these images, by which it is possible to identify the longest blob across all filter outputs, identified as the 'path'.

line in Fig. 3b) results in only a modest decrement of performance for human foveal vision (filled symbols in Fig. 3b), adding weight to the suggestion that linking processes between cells tuned to different orientations are necessary to explain foveal contour integration.

Evaluation of peripheral visual function with the same stimuli produces a very different conclusion. Figure 3c shows results for a range of eccentric loci in the visual field (10°, 20°, 25°, and 30° into the temporal retina). Path detection is constant over a wide range of viewing distances (the task exhibits scale invariance) as seen from the correspondence of data when using stimuli differing in scale by a factor of eight (Fig. 3c). This obviates the need to scale stimuli to allow for known variation in cortical magnification across the visual field. Furthermore, by using an orientation-discrimination task we ensured that the carrier frequency of our patterns was below the Nyquist limit at the largest eccentricity tested[9]. Our results reveal not only a reduction in peripheral performance for larger path angles but also invariant performance beyond about 10° eccentricity. The known differences between fovea and periphery cannot account for the latter finding, but our model of the filtering properties of individual cortical cells (Fig. 3c) is sufficient to explain peripheral performance. Furthermore, beyond 10° eccentricity, paths composed of elements with randomly alternating phase are undetectable (Fig. 3d), indicating that peripheral paths might be seen using no more than filtering operations (solid line in Fig. 3d shows predictions of such a model). This conclusion is also supported by subjects' reported perception that peripheral paths, unlike their foveal counterparts, appear perceptually smeared along their length (sometimes described by subjects as 'creases').

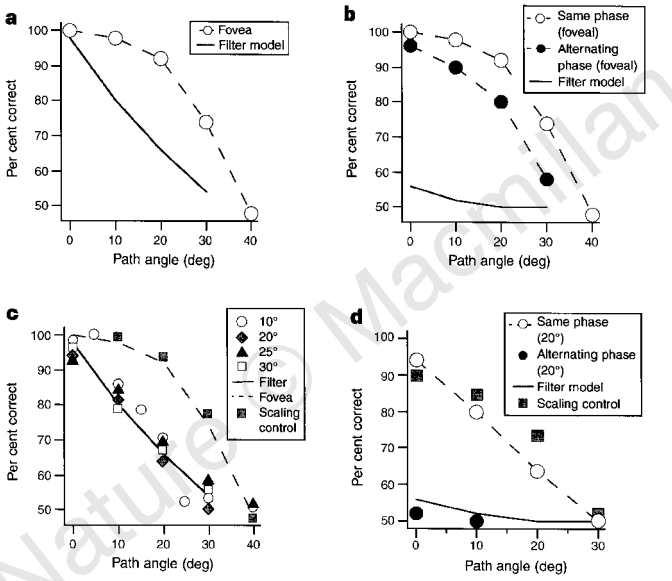

Figure 3 Detection of paths embedded in a background field of randomly oriented elements. Performance (% correct choices) is plotted as a function of path angle. In each frame human performance is compared with the performance of the 'simple-filter' model in which there is no integration across filters tuned to different orientations. **a**, Foveal performance is compared with that of the simple-filter model. **b**, Foveal performance is compared for elements with alternating spatial phase with that of the filtering model. For comparison human performance for elements with the same spatial phase is shown. **c**, Human performance (with the same stimuli as in **a**) for a range of eccentric loci in the visual field (10°, 20°, 25°, 30°) is compared with the predictions of the filtering model. Foveal performance is shown at two different scales (dashed line: carrier is 3 cycles per degree (c.p.d.) shaded squares: carrier is 24 c.p.d.), demonstrating scale invariance, so decreased performance in the periphery cannot be due to its coarser neural sampling. **d**, Peripheral performance for 20° eccentricity is compared for elements with alternating spatial phase with that of the filtering model. For comparison human performance at the 20° locus for elements having the same spatial phase is shown. Squares indicate foveal performance with an alternating phase path which has been scaled (carrier is 24 c.p.d) to reflect the decrease in neural sampling at 20° eccentricity. Poor performance with alternating phase paths in the periphery is clearly not attributable to a scaling difference between fovea and periphery.

The need for substantial interaction between cells tuned to different orientations to integrate the distributed neuronal activity for the definition of simple contours carries with it a substantial commitment of cortical resources. Our finding indicates that the human visual system might limit such interactions to central vision. In the periphery, the visual system relies more on simple filtering operations at independent orientations to define contours, representing a substantial economy in cortical processing. It has long been argued that foveal and peripheral processing occur along quite different lines[2,3], the former involving discrimination, the latter detection. But to date, the only quantitative differences found between foveal and peripheral visual processing have involved contrast thresholds and spatial scale, neither of which could support such a claim. A difference in the way contours are defined could form the computational basis of such a claim. Recent attempts to understand the physiological basis of contour binding have implicated the long-range cortical interactions observed anatomically[10] and physiologically[11], and the synchronization of cortical oscillations observed physiologically[4–7]. Whatever the physiological basis, in the light of our results, it should be limited to the central visual field. □

Methods

Psychophysics. Paths had a backbone of eight invisible line segments; each line segment was of the same length and joined other segments at an angle uniformly distributed between $+\alpha$ and $-\alpha$, where α is the path angle[1] and varies from $\alpha = 0°$ (straight) to $\alpha = 40°$ (very curved). Subjects were shown two images in random order on each of 100 presentations, one containing just the background elements and another containing a path embedded in a field of background elements. Element density was the same in these two presentations. Subjects were asked to select the presentation containing the path. The elements were narrowband in spatial frequency and orientation, and were displayed at a contrast of 90%, all being in sine phase for a duration of 1 s. The carrier of the Gabor patches was set to 3 cycles per degree, the gaussian envelope had $\sigma = 8$ arc min. and the inter-element spacing as 3.35 times the carrier period.

Computational model. Images were initially convolved with a bank of 12 spatial filters oriented from 0°–165° in steps of 15°. Filters had a peak spatial frequency matched to the carrier component of the Gabor patches comprising the stimulus. As long as the filter is band-limited in the spatial-frequency and orientation domains, its exact form is unimportant. We used two-dimensional difference-of-gaussian (DoG) filters composed of a DoG in the x direction multiplied by a gaussian function in the y direction:

$$W(x,y) = \left[\exp(-x_t^2/2\sigma^2) - \frac{1}{1.23}\exp(-x_t^2/2(2.23\sigma)^2)\right]\exp(-y_t^2/2(3\sigma)^2)$$

where σ refers to the standard deviation of the positive gaussian function and (x_t, y_t) are coordinates rotated by angle ϕ:

$$x_t = x\cos\phi + y\sin\phi$$

$$y_t = y\cos\phi - x\sin\phi$$

Parameters of the DoG are based on those derived in ref. 12.

Filter output is 'thresholded' by setting all grey levels falling within ± 1 standard deviation of the mean to the mean value itself. The thresholding operation serves to reduce the effect of noise and to avoid production of very large or complex two-dimensional 'blobs'. A symbolic description of each of these 'blobs' is generated as a list of parameters describing the position, orientation, length, width, and so on[13]. By selecting the longest blob across all filter orientations, embedded contours may be detected (if orientation differences between adjacent components are sufficiently small). To compare the predictions of this model to human data, we used a procedure for generating

stimuli similar to that used for the psychophysical experiment. Pairs of textures either containing or not containing an embedded contour were generated and processed using the model. The longest blob was calculated for both images, and the image producing the longer of the two was selected as the one containing the contour. Performance of the model was determined as a function of path angle (the orientational difference between successive elements of the contour).

Received 9 May; accepted 9 September 1997.

1. Field, D. J., Hayes, A. & Hess, R. F. Contour integration by the human visual system: evidence for a local "association field". *Vision Res.* **33,** 173–193 (1993).
2. Aubert, H. & Foerster, E. Unter suchungen über raumsinn der retina. *Albrecht v. Graefes Arch. Opthalmol.* **3,** 1–37 (1857).
3. Schneider, G. E. Two visual systems. *Science* **163,** 895–902 (1969).
4. von der Malsburg, C. in *Synergetics of the Brain* (ed. Basar, E., Flohr, H., Haken, H. & Mandall, A. J.) 238–249 (Springer, Berlin, 1983).
5. von der Malsburg, C. & Singer, W. in *Neurobiology of Neocortex* (eds Rakic, P. & Singer, W.) 69–99 (Wiley, Chichester, 1988).
6. Kreiter, A. K. & Singer, W. Global stimulus arrangement determines synchronization of neuronal activity in the awake macaque monkey. *Eur. J. Neurosci.* (suppl.) **7,** 153 (1994).
7. Engel, A. K., Konig, P., Kreiter, A. K., Schillen, T. B. & Singer, W. Temporal coding in the visual cortex: new vistas on integration in the nervous system. *Trends Neurosci.* **15,** 218–226 (1992).
8. Watt, R. J. & Morgan, M. J. A theory of the primitive spatial code in human vision. *Vis. Res.* **25,** 1661–1674 (1985).
9. Wang, Y., Thibos, L. N. & Bradley, A. Undersampling produces non-veridical motion perception, but not necessarily motion reversal, in peripheral vision. *Vision Res.* **36,** 1737–1744 (1996).
10. Gilbert, C. D. & Wiesel, T. N. Columnar specificity of intrinsic horizontal and corticocortical connections in cat visual cortex. *J. Neurosci.* **9,** 2432–2442 (1989).
11. Tso, D. Y. & Gilbert, C. D. The organization of chromatic and spatial interactions in the primate striate cortex. *J. Neurosci.* **8,** 1712–1727 (1988).
12. Phillips, G. & Wilson, H. Orientation bandwidths of spatial mechanisms measured by masking. *J. Opt. Soc. Am.* **62,** 226–232 (1983).
13. Watt, R. J. *Understanding Vision* (Academic, London, 1991).

Acknowledgements. This work was supported by the Canadian MRC (MT 10818).

Correspondence and requests for materials should be addressed to R.F.H. (e-mail: rhess@bradman.vision.mcgill.ca)

Fear conditioning induces associative long-term potentiation in the amygdala

Michael T. Rogan, Ursula V. Stäubli & Joseph E. LeDoux

Center for Neural Science, New York University, 6 Washington Place, New York, New York 10003, USA

Long-term potentiation (LTP) is an experience-dependent form of neural plasticity believed to involve mechanisms that underlie memory formation[1–3]. LTP has been studied most extensively in the hippocampus, but the relation between hippocampal LTP and memory has been difficult to establish[4–6]. Here we explore the relation between LTP and memory in fear conditioning, an amygdala-dependent form of learning in which an innocuous conditioned stimulus (CS) elicits fear responses after being associatively paired with an aversive unconditioned stimulus (US). We have previously shown that LTP induction in pathways that transmit auditory CS information to the lateral nucleus of the amygdala (LA) increases auditory-evoked field potentials in this nucleus[7]. Now we show that fear conditioning alters auditory CS-evoked responses in LA in the same way as LTP induction. The changes parallel the acquisition of CS-elicited fear behaviour, are enduring, and do not occur if the CS and US remain unpaired. LTP-like associative processes thus occur during fear conditioning, and these may underlie the long-term associative plasticity that constitutes memory of the conditioning experience.

To determine whether fear conditioning results in learning-related changes in CS processing that are similar to the effect of LTP induction in auditory CS pathways, we concurrently measured auditory CS-evoked field potentials in LA and CS-evoked fear behaviour, before, during and after fear conditioning in freely behaving rats. The rats were randomly assigned to groups that underwent either fear conditioning (in which the CS and US were paired) or a non-associative control procedure (in which the CS and US were explicitly unpaired). The CS was a 20-s series of acoustic tones (1 kHz, 50 ms, 72 dB) delivered at 1 Hz. The onset of each tone in the series triggered the acquisition of an evoked waveform from the electrode in LA, so that each 20-s CS produced 20 evoked responses. The 100 evoked waveforms from each session (5 CS per session; mean inter-CS interval, 170 s, range 140–200 s) were averaged to yield a mean CS-evoked field potential (CS-EP) for that session. The use of this 'one tone per second' 20-s CS allowed the sampling of CS-evoked activity at 20 points within a single CS, greatly increasing the signal-to-noise ratio of the field potentials under study over that obtainable with the continuous-tone CS typically used in conditioning studies[8–10].

The CS-EPs were quantified by measuring the latency, slope and amplitude of the negative-going potential occurring 15–30 ms after the onset of the tone stimulus, as per our previous study of auditory evoked field potentials in LA[7]. Anatomical and physiological evidence indicates that these field potentials are generated in the LA[6]. A set of CS-EPs for two rats, one from the 'conditioned' group and one from the 'control' group, over the seven sessions of testing and training is shown in Fig. 1a. As previously reported[7], before training the CS elicited a negative-going field potential with a latency of about 18 ms (18.52 ± 3.58 ms across animals). The raw (not normalized) slope and amplitude of these potentials did not differ between the two groups in the baseline tests before training (slope: conditioned group, $-1.649 \pm .425\ \mu V\ ms^{-1}$, control group, $-2.329 \pm .346\ \mu V\ ms^{-1}$; *t*-test, $P > 0.05$, conditioned group, $14.186 \pm 4.103\ \mu V$; control group, 18.116 ± 4.214; *t*-test, $P > 0.05$). As seen in the examples shown (Fig. 1a), paired training led to an increase in the slope and amplitude of the CS-EPs, whereas unpaired training did not. Mean group data of slope and amplitude of CS-EPs, normalized as a percentage of mean baseline measures, are shown in Fig. 1b. For both groups, slope and amplitude were stable for the first two sessions (testing), in which only the CS was presented. Responses in these sessions were used as a baseline from which to measure changes due to training. For the conditioned group, slope and amplitude were unchanged by unpaired presentations of the CS and US in session 3, but increased significantly above baseline in sessions 4 and 5 when the CS was paired with the US (statistics in Fig. 1b). Both measures remained elevated in session 6, in which only the CS was presented, and fell towards baseline in the last session, reflecting the weakening of the CS-US relation by presentations of the CS without the US (extinction trials). The slope and amplitude of the CS-EPs remained statistically unchanged throughout the course of training and testing for the control group (statistics in Fig. 1b). Slope and amplitude did not differ between the groups until pairing occurred, and remained different until the last session (statistics in Fig. 1b). The fact that the two groups received an equal number of CS and US presentations during training, and that unpaired training was not accompanied by increases in CS-EPs in either group, indicates that the effect of paired training on the field potentials in the conditioned group is due to the associative relation of the CS and US and not to nonspecific arousal elicited by either stimulus alone[11].

The differential effects of training on CS-EPs for each member of the control and conditioned groups is shown in Fig. 2. This scattergram demonstrates the consistency with which the control group was unaffected by training and the reliability of the increases in slope and amplitude of the CS-EPs in the conditioned group.

The acquisition of conditioned fear behaviour was evaluated by measuring 'freezing', a characteristic defensive posture expressed in the presence of stimuli that predict danger[12–15]. The amount of time accounted for by freezing was measured during the 20-s CS and also during the 20 s immediately before CS onset (pre-CS period). The latter is a measure of the acquisition of aversive conditioning to the experimental context in which the US is delivered (such as the conditioning chamber); freezing to the experimental context is